

## Amide-I and -II Vibrations of the Cyclic $\beta$ -Sheet Model Peptide Gramicidin S in the Gas Phase

Peter Kupser,<sup>†</sup> Kevin Pagel,<sup>‡,§</sup> Jos Oomens,<sup>||</sup> Nick Polfer,<sup>||,⊥</sup> Beate Kokschi,<sup>‡</sup>  
Gerard Meijer,<sup>†</sup> and Gert von Helden<sup>\*,†</sup>

*Fritz-Haber-Institut der Max-Planck-Gesellschaft, Faradayweg 4-6, 14195 Berlin, Germany, Institut für Chemie und Biochemie, Freie Universität Berlin, Takustrasse 3, 14195 Berlin, Germany, and FOM Institute for Plasmaphysics, Edisonbaan 14, 3439 MN Nieuwegein, The Netherlands*

Received November 20, 2009; E-mail: helden@fhi-berlin.mpg.de

**Abstract:** In the condensed phase, the peptide gramicidin S is often considered as a model system for a  $\beta$ -sheet structure. Here, we investigate gramicidin S free of any influences of the environment by measuring the mid-IR spectra of doubly protonated (deuterated) gramicidin S in the gas phase. In the amide I (i.e., C=O stretch) region, the spectra show a broad split peak between 1580 and 1720  $\text{cm}^{-1}$ . To deduce structural information, the conformational space has been searched using molecular dynamics methods and several structural candidates have been further investigated at the density functional level. The calculations show the importance of the interactions of the charged side-chains with the backbone, which is responsible for the lower frequency part of the amide I peak. When this interaction is inhibited via complexation with two 18-crown-6 molecules, the amide I peak narrows and shows two maxima at 1653 and 1680  $\text{cm}^{-1}$ . A comparison to calculations shows that for this complexed ion, four C=O groups are in an antiparallel  $\beta$ -sheet arrangement. Surprisingly, an analysis of the calculated spectra shows that these  $\beta$ -sheet C=O groups give rise to the vibrations near 1680  $\text{cm}^{-1}$ . This is in sharp contrast to expectations based on values for the condensed phase, where resonances of  $\beta$ -sheet sections are thought to occur near 1630  $\text{cm}^{-1}$ . The difference between those values might be caused by interactions with the environment, as the condensed phase value is mostly deduced for  $\beta$ -sheet sections that are embedded in larger proteins, that interact strongly with solvent or that are part of partially aggregated species.

### Introduction

The function of biological molecules is determined by their three-dimensional structure and shape. For peptides and proteins, these three-dimensional structures are the consequence of the primary sequences of amino acids, the resulting intrinsic intramolecular interactions as well as the interactions of the molecules with their environments. The main interactions include bond stretching, angle bending and twisting terms, as well as intra- and intermolecular repulsive, dispersive and electrostatic interactions. The subtle balance between all those intra- and intermolecular interactions gives rise to extremely complex potential energy surfaces in the folding of biological molecules, such as proteins. Traditionally, studies on biological molecules are performed in the condensed phase, where information directly relevant to the structure of the molecule under physiological conditions is obtained. However, to get an in-depth understanding of the individual contributions to the potential energy landscape, the structures of peptides and proteins can be investigated in the gas phase and therefore in the absence of solvent effects.

Initial experiments on biological molecules in the gas phase were performed on neutral species in molecular beams.<sup>1</sup> The molecules can be brought into the gas phase by either thermal evaporation or laser desorption. The former technique is limited to small, thermally stable species while laser desorptions also allows for the investigation of larger species such as neutral gramicidin peptides.<sup>2</sup> Over the last years, several techniques have been developed to allow for studies of large, charged biomolecules in the gas phase. However, obtaining structural (or dynamic) information on such molecules is difficult. For condensed phase samples, numerous spectroscopic and scattering techniques exist. For gas-phase species choices are more limited. Two techniques that deliver direct structural information are gas-phase ion mobility measurements<sup>3–5</sup> and infrared spectroscopy.

- (1) Rizzo, T.; Park, Y.; Peteanu, L.; Levy, D. *J. Chem. Phys.* **1986**, *84*, 2534–2541.
- (2) Abo-Riziq, A.; Crews, B. O.; Callahan, M. P.; Grace, L.; de Vries, M. S. *Angew. Chem., Int. Ed.* **2006**, *45*, 5166–5169.
- (3) von Helden, G.; Wytttenbach, T.; Bowers, M. T. *Science* **1995**, *267*, 1483–1485.
- (4) Clemmer, D. E.; Jarrold, M. F. *J. Mass Spectrom.* **1997**, *32*, 577–592.
- (5) Wytttenbach, T.; Bowers, M. T. *Annu. Rev. Phys. Chem.* **2007**, *58*, 511–533.
- (6) Oh, H.; Breuker, K.; Sze, S. K.; Ge, Y.; Carpenter, B. K.; McLafferty, F. W. *Proc. Natl. Acad. Sci. U.S.A.* **2002**, *99*, 15863–15868.
- (7) Oomens, J.; Polfer, N.; Moore, D. T.; van der Meer, L.; Marshall, A. G.; Eyler, J. R.; Meijer, G.; von Helden, G. *Phys. Chem. Chem. Phys.* **2005**, *7*, 1345–1348.

<sup>†</sup> Fritz-Haber-Institut.

<sup>‡</sup> Freie Universität Berlin.

<sup>§</sup> Current address: University of Cambridge, Department of Chemistry, Lensfield Road, Cambridge, CB2 1EW, U.K.

<sup>||</sup> FOM Institute.

<sup>⊥</sup> Current address: Department of Chemistry, University of Florida, Gainesville, FL 32611.

copy.<sup>6–8</sup> These two techniques are rather complementary, as ion mobility probes the overall shape and is not very sensitive to the local structure whereas IR spectroscopy probes the bonds between the atoms and is not as sensitive to the overall structure.

For small gas-phase biomolecules, mid-IR spectroscopy has in many instances shown to yield detailed structural information.<sup>9–15</sup> This is especially true when the molecules are internally cold and when individual oscillators give rise to individual peaks. A comparison with theoretical predictions can then give detailed structural information. For larger systems, the situation is more complicated as resonances from individual oscillators overlap and give rise to a broad envelope.<sup>7</sup> When the samples are warm, several mechanisms can cause peak broadening and the possible presence of several conformers can result in overlapping spectra of different species. Further, theory is becoming increasingly difficult when the size of the system increases. For condensed phase proteins, IR spectroscopy is a standard technique to determine secondary structures and even small changes in peak shapes and position can be attributed to structural changes.<sup>16</sup> In part, this is possible because an extended database of condensed-phase IR spectra has been recorded for proteins with known secondary structures. This has allowed a structure-spectrum correlation, where diagnostic band positions, notably the amide I band (C=O stretching vibration), are used to make a structural identification.

In the condensed phase,  $\alpha$ -helices as well as disordered structures have amide-I band positions near 1654  $\text{cm}^{-1}$ , while  $\beta$ -sheet type structures have band positions near 1633  $\text{cm}^{-1}$ .<sup>16</sup> However, the environment can have a strong influence on those values. For example, in a study on a  $\beta$ -hairpin peptide, for which it was shown by NMR that its structure is folded,  $\beta$ -sheet-like, the amide-I modes are found centered around 1640 and 1670  $\text{cm}^{-1}$ , at identical positions to those of a reference peptide having a random coil structure.<sup>17</sup> Only at high concentrations, when the peptides start to aggregate, does an additional peak near 1616  $\text{cm}^{-1}$  appear. IR studies on the cyclic peptide gramicidin S highlight the important role of the environment as well.<sup>18</sup> In polar protic solvents, the main amide I band is found near 1629  $\text{cm}^{-1}$ , however it is observed to shift when the protic character of the solvent is reduced and for dimethyl sulfoxide (DMSO), an amide I position of 1652  $\text{cm}^{-1}$  is observed while the secondary structure of the peptide is assumed not to change.<sup>18</sup> The spectral signatures of  $\beta$ -sheet peptides can thus be highly dependent on the environment.

For peptides and proteins in the gas phase, no database which correlates structure to spectra is available. It is thus important

to investigate in the gas phase medium to large size model systems with well-defined structures to establish the corresponding mid-infrared signatures and compare them to the spectral signatures of large proteins,<sup>7</sup> small neutral model systems for  $\beta$ -sheet structures,<sup>9,11–13,15</sup> helices,<sup>19</sup> turns<sup>14</sup> and to data from the condensed phase. While for small neutral species, model systems for  $\beta$ -sheet structures were investigated,<sup>9,11–13,15,20</sup> the search for the presence of such structures in charged species in the gas phase remained elusive so far.<sup>20,21</sup> However, understanding the spectral signatures of charged,  $\beta$ -sheet rich systems in the gas phase is of tremendous importance since it might pave the way for a variety of future experiments where IR spectrometry is combined with mass spectrometric techniques. In contrast to most condensed-phase techniques, MS-based approaches are capable of analyzing specific species within an ensemble of enormous inherent heterogeneity. The IR-MS combination, therefore, exhibits an outstanding potential to obtain information about the secondary structure of the toxic, but still poorly characterized oligomers that precede fibril formation of proteins involved in a variety of amyloid diseases.<sup>22</sup>

Due to internal constraints, the cyclic peptide gramicidin S (GramS) could serve as a model for a  $\beta$ -sheet structure even for charged species. Gramicidin S was discovered in the 1940s in the former Soviet Union as a substance with antibiotic character that is produced by *Bacillus brevis*.<sup>23</sup> Subsequent characterization revealed its amino acid sequence.<sup>24</sup> Its structure is proposed to consist of an antiparallel  $\beta$ -sheet, stabilized by four intramolecular hydrogen bonds between two opposing leucine and valine residues and two  $\beta$ -turns consisting of two D-phenylalanine and proline residues.<sup>25</sup> In addition, gramicidin S contains two ornithine groups that have basic side-chains (see Figure 1). Gramicidin S and derivatives have been extensively studied in the condensed phase. As gramicidin S is difficult to crystallize, comparatively few X-ray crystallography studies exist. X-ray structural characterization has been performed on the hydrated gramicidin S–urea complex<sup>26</sup> as well as on a derivative in which the Orn and Phe peptidic nitrogen atoms are methylated and in which the side-chain of Orn contains a protecting group.<sup>27</sup> In these studies, the proposed antiparallel  $\beta$ -sheet structure is found with additional interactions of the Orn side-chains with the D-Phe C=O groups. In case of the urea complex, only one side-chain is found to be involved in this interaction,<sup>26</sup> while in the other study both side-chains are found to interact.<sup>27</sup> There are two possibilities how this interaction can take place. In the hydrated gramicidin S–urea complex,<sup>26</sup> the side-chain is found to form an H-bond to  $i \rightarrow i+2$  Phe C=O (the nearest Phe clockwise in Figure 1) and in the study on the derivative, this interaction is found to occur to the  $i \rightarrow i-3$  Phe residue (counterclockwise in Figure 1). Many

(8) Polfer, N. C.; Oomens, J. *Mass Spectrom Rev.* **2009**, *28*, 468–494.

(9) Gerhards, M.; Unterberg, C.; Gerlach, A. *Phys. Chem. Chem. Phys.* **2002**, *4*, 5563–5565.

(10) Bakker, J.; Mac Aleese, L.; Meijer, G.; von Helden, G. *Phys. Rev. Lett.* **2003**, *91*, 203003.

(11) Gerhards, M.; Unterberg, C.; Gerlach, A.; Jansen, A. *Phys. Chem. Chem. Phys.* **2004**, *6*, 2682–2690.

(12) Gerlach, A.; Unterberg, C.; Fricke, H.; Gerhards, M. *Mol. Phys.* **2005**, *103*, 1521–1529.

(13) Fricke, H.; Gerlach, A.; Gerhards, M. *Phys. Chem. Chem. Phys.* **2006**, *8*, 1660–1662.

(14) Compagnon, I.; Oomens, J.; Meijer, G.; von Helden, G. *J. Am. Chem. Soc.* **2006**, *128*, 3592–3597.

(15) Fricke, H.; Funk, A.; Schrader, T.; Gerhards, M. *J. Am. Chem. Soc.* **2008**, *130*, 4692–4698.

(16) Barth, A. *Biochim. Biophys. Acta* **2007**, *1767*, 1073–1101.

(17) Colley, C. S.; Griffiths-Jones, S. R.; George, M. W.; Searle, M. S. *Chem. Commun.* **2000**, 593–594.

(18) Lewis, R. N. A. H.; Prenner, E. J.; Kondejewski, L. H.; Flach, C. R.; Mendelsohn, R.; Hodges, R. S.; McElhaney, R. N. *Biochemistry* **1999**, *38*, 15193–15203.

(19) Pagel, K.; Kupser, P.; Bierau, F.; Polfer, N. C.; Steill, J. D.; Oomens, J.; Meijer, G.; Koksche, B.; von Helden, G. *Int. J. Mass Spectrom.* **2009**, *283*, 161–168.

(20) Dugourd, P.; Antoine, R.; Breaux, G.; Broyer, M.; Jarrold, M. F. *J. Am. Chem. Soc.* **2005**, *127*, 4675–4679.

(21) Jarrold, M. F. *Phys. Chem. Chem. Phys.* **2007**, *9*, 1659–1671.

(22) Bernstein, S. L.; Dupuis, N. F.; Lazo, N. D.; Wyttenbach, T.; Condron, M. M.; Bitan, G.; Teplow, D. B.; Shea, J. E.; Ruotolo, B. T.; Robinson, C. V.; Bowers, M. T. *Nature Chem.* **2009**, *1*, 326–331.

(23) Gause, G. F.; Brazhnikova, M. G. *Nature* **1944**, *154*, 703.

(24) Syngé, R. L. M. *Biochem. J.* **1945**, *39*, 363–367.

(25) Hodgkin, D. C.; Oughton, B. M. *Biochem. J.* **1957**, *65*, 752–756.

(26) Hull, S. E.; Karlsson, R.; Main, P.; Woolfson, M. M.; Dodson, E. J. *Nature* **1978**, *275*, 206–207.

(27) Yamada, K.; Unno, M.; Kobayashi, K.; Oku, H.; Yamamura, H.; Araki, S.; Matsumoto, H.; Katakai, R.; Kawai, M. *J. Am. Chem. Soc.* **2002**, *124*, 12684–12688.

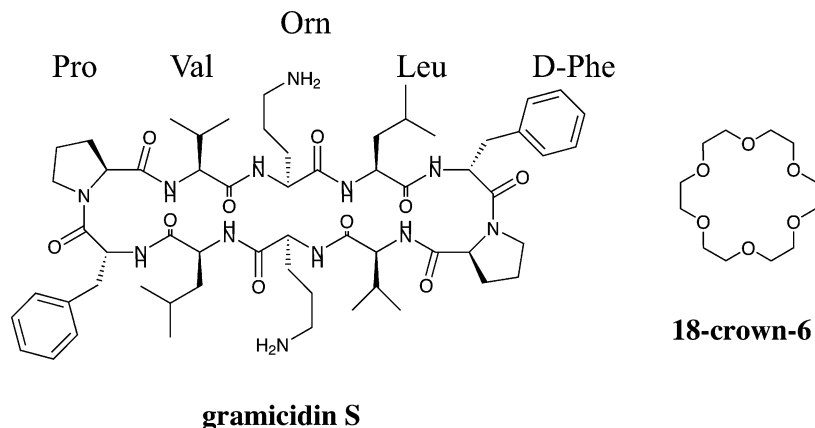


**Figure 1.** Cyclic decapeptide gramicidin S (cyclo(Pro-Val-Orn-Leu-D-Phe)<sub>2</sub>) and the crown-ether 18-crown-6.

NMR studies on gramicidin S and its derivatives have been carried out. The backbone is generally found to adopt the antiparallel pleated  $\beta$ -sheet conformation.<sup>28–31</sup> The Orn side-chains are found to adopt the  $i \rightarrow i+2$  configuration,<sup>28,30</sup> however, in one study, a combination of both orientations<sup>29</sup> is found. Gramicidin S is also investigated in the gas phase as a charged molecule using mass spectrometric methods,<sup>32–34</sup> and from ion mobility studies, it is concluded that a  $\beta$ -sheet structure is present.<sup>34</sup> Spectroscopic studies on neutral gas-phase gramicidin S in the X–H stretching region give a N–H stretching signature that is compatible with a  $\beta$ -sheet structure as well.<sup>2</sup> Here, we present a mid-IR study of doubly protonated gramicidin S in the gas phase.

## Experimental Section

The experiments were performed using the Fourier-transform ion cyclotron resonance (FT-ICR) mass spectrometer at the free electron laser facility FELIX in Nieuwegein, The Netherlands.<sup>35</sup> Gramicidin S was synthesized in the group of A.S. Ulrich.<sup>36</sup> It was dissolved at a 50  $\mu$ M concentration in a H<sub>2</sub>O/methanol/AcOH solution of 60/39/1%. In some experiments, 18-crown-6 ether was added at a concentration of 200  $\mu$ M. The solution was sprayed using a Z-Spray electrospray source (Micromass, Manchester, UK) and the ions were transferred to the ICR trapping cell. Deuteration was performed by dissolving gramicidin S in deuterated solvents. The observed mass increases by 14 amu, indicating that all exchangeable hydrogen atoms were replaced by deuterium. After isolation of the mass/charge ratio of interest, the ions were irradiated for a few seconds by the IR output of the free electron laser FELIX. When the IR frequency of the light is resonant with an IR active vibration of the ions, the sequential absorption of many photons and subsequent fragmentation (infrared multiple photon dissociation (IRMPD))

occurs. IR spectra can be recorded by monitoring the fragmentation yield as a function of IR wavelength. Although the so obtained spectra are not identical to linear IR absorption spectra, it was shown that they can be very close to them.<sup>37</sup>

As IR light source, the free electron laser FELIX<sup>38</sup> was used. It is continuously tunable over the 5–250  $\mu$ m range. The light output comes in macropulses of about 5  $\mu$ s length at a repetition frequency of up to 10 Hz (5 Hz is used in the present experiment). The macropulses contain micropulses which can be adjusted in length between 300 fs and several ps. The bandwidth is transform limited and can range from 0.5% fwhm of the central wavelength to several percent. The micropulse repetition rate can be selected to be either 25 MHz or 1 GHz, resulting in a micropulse spacing of 40 or 1 ns, respectively. In the 1 GHz mode, the output energy can be up to 100 mJ/macropulse.

## Results

**Measured IR Spectra.** When the IR radiation of FELIX is resonant with an IR active vibrational mode of the molecule, IRMPD can be observed. For the here investigated doubly protonated gramicidin S, fragmentation is observed to be distributed over a multitude of different fragmentation channels and the corresponding total ion intensity in each of those channels individually can be quite low. As a consequence, instead of monitoring the appearance of fragment ions, the depletion of parent ions is monitored.

In the top part of Figure 2, the gas-phase IR spectra of [GramS + 2H]<sup>2+</sup> as well as of perdeuterated [d-GramS + 2D]<sup>2+</sup> are shown. The spectrum of [GramS + 2H]<sup>2+</sup> shows a broad split peak between 1580 and 1720  $\text{cm}^{-1}$ , another intense peak around 1500  $\text{cm}^{-1}$  and some less intense structure between 1300 and 1410  $\text{cm}^{-1}$ . The split peak is in the region where one expects the amide-I (C=O stretch) vibration to occur while the peak at 1500  $\text{cm}^{-1}$  is where the amide-II (N–H bending) vibration is expected to be present. The IR spectrum of [d-GramS + 2D]<sup>2+</sup> between 1580 and 1720  $\text{cm}^{-1}$  shows a structure consisting of at least three underlying peaks. The peak observed for [GramS + 2H]<sup>2+</sup> near 1500  $\text{cm}^{-1}$  appears to be changed in shape and shifted to  $\sim 1410 \text{ cm}^{-1}$ .

Assuming pure amide-I and -II vibrations to be present in the molecule, one would expect essentially no change in shape for the amide-I band upon deuteration. A small shift of this band of 1–5  $\text{cm}^{-1}$  can be due to coupling of the C=O stretch

(28) Krauss, E. M.; Chan, S. I. *J. Am. Chem. Soc.* **1982**, *104*, 6953–6961.

(29) Xu, Y.; Sugár, I. P.; Krishna, N. R. *J. Biomol. NMR* **1995**, *5*, 37–48.

(30) Kawai, M.; Yamamoto, T.; Yamada, K.; Yamaguchi, M.; Kurobe, S.; Yamamura, H.; Araki, S.; Butsugan, Y.; Kobayashi, K.; Kataaki, R.; Saito, K.; Nakajima, T. *Lett. Pept. Sci.* **1998**, *5*, 5–12.

(31) Gibbs, A. C.; Kondejewski, L. H.; Gronwald, W.; Nip, A. M.; Hodges, R. S.; Sykes, B. D.; Wishart, D. S. *Nat. Struct. Bio.* **1998**, *5*, 284–288.

(32) Gross, D. S.; Williams, E. R. *J. Am. Chem. Soc.* **1996**, *118*, 202–204.

(33) Rodriguez-Cruz, S. E.; Klassen, J. S.; Williams, E. R. *J. Am. Soc. Mass Spectrom.* **1997**, *8*, 565–568.

(34) Ruotolo, B. T.; Tate, C. C.; Russell, D. H. *J. Am. Soc. Mass Spectrom.* **2004**, *15*, 870–878.

(35) Valle, J. J.; Eyler, J. R.; Oomens, J.; Moore, D. T.; van der Meer, A. F. G.; von Helden, G.; Meijer, G.; Hendrickson, C. L.; Marshall, A. G.; Blakney, G. T. *Rev. Sci. Instrum.* **2005**, *76*, 023103.

(36) Wadhvani, P.; Afonin, S.; Ieromino, M.; Buerck, J.; Ulrich, A. S. *J. Org. Chem.* **2006**, *71*, 55–61.

(37) Oomens, J.; Sartakov, B. G.; Meijer, G.; von Helden, G. *Int. J. Mass Spectrom.* **2006**, *254*, 1–19.

(38) Oepts, D.; van der Meer, A. F. G.; van Amersfoort, P. W. *Infrared Phys. Tech.* **1995**, *36*, 297–308.

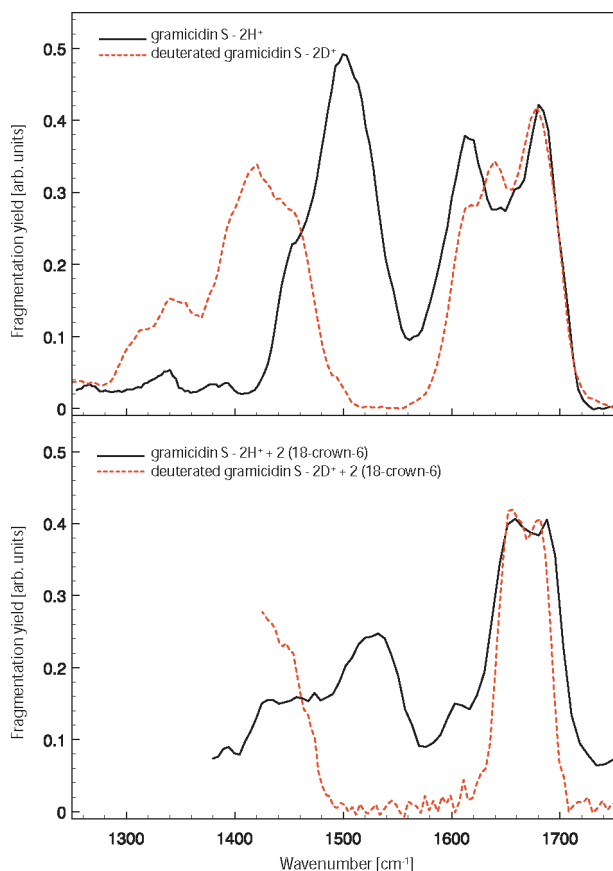


**Figure 2.** (Top) Experimental IR spectra of  $[\text{GramS} + 2\text{H}]^{2+}$  and deuterated  $[\text{d-GramS} + 2\text{D}]^{2+}$ . (Bottom) Experimental IR spectrum of  $[\text{GramS} + 2\text{H}]^{2+}$  complexed with two 18-crown-6 molecules and perdeuterated  $[\text{d-GramS} + 2\text{D}]^{2+}$ , complexed with two 18-crown-6 molecules. Amide-I ( $\text{C}=\text{O}$  stretch) vibrations are expected to be found above  $1600\text{ cm}^{-1}$ .

motion with the  $\text{N}-\text{H}$  ( $\text{N}-\text{D}$ ) in plane bending motion. The amide-II band on the other hand consists to a large extent of  $\text{N}-\text{H}$  bending motion and in solution, it can be found near  $1550\text{ cm}^{-1}$ . Upon deuteration, the mode shifts to  $1460\text{--}1490\text{ cm}^{-1}$  and is then termed amide-II'. It also changes its character and consists to a large extent of  $\text{C}-\text{N}$  stretching motion in deuterated molecules.

When comparing the two spectra in the top part of Figure 2, the expected isotopic shift in the amide-II band can be clearly observed. At first glance surprising, however, might be the change in peak shape in the amide-I region, as it implies that this structure is not solely due to  $\text{C}=\text{O}$  stretching motion. On the other hand, looking at the structure of the molecule and considering the fact that we are looking at the doubly protonated cation, it is also clear that a simple picture of pure amide-I and -II vibration does not hold. The two protons (deuterons) will attach to the most basic sites in the molecule, the two ornithine side-chains (see Figure 1), and the  $-(\text{CH}_2)_3\text{-NH}_3^+$  side-chains will then coordinate to backbone  $\text{C}=\text{O}$  groups. The resulting strong hydrogen bonds can then significantly shift the frequency of those  $\text{C}=\text{O}$  oscillators. In addition, the  $-\text{NH}_3^+$  groups by themselves are IR active and give for lysine in solution a  $\delta_{\text{as}}$  mode around  $1627\text{ cm}^{-1}$  and a  $\delta_{\text{s}}$  mode around  $1526\text{ cm}^{-1}$ .<sup>16</sup> Upon deuteration, those modes then shift to  $1201$  and  $1170\text{ cm}^{-1}$ , respectively.<sup>16</sup> This is in line with the observation that the red side of the structure in the amide-I region in the spectrum

of  $[\text{GramS} + 2\text{H}]^{2+}$ , where the  $\delta_{\text{as}}$  mode of  $-\text{NH}_3^+$  is expected, undergoes the largest change upon deuteration.

For a further investigation of the effect of the charged side-chain and, in particular, to study the peptidic backbone with reduced backbone–side-chain interaction, experiments were performed in which  $[\text{GramS} + 2\text{H}]^{2+}$  is complexed with two 18-crown-6 molecules. These crown ether molecules have a very high affinity to protonated amines<sup>39</sup> and it is expected that in such a complex, the side-chain  $-\text{NH}_3^+$  groups are coordinated to 18-crown-6 molecules and that the interaction of the  $-\text{NH}_3^+$  groups to the backbone is inhibited due to steric constraints.

The bottom part of 2 shows the IR spectra of  $[\text{GramS} + 2\text{H}]^{2+}$  and of deuterated  $[\text{d-GramS} + 2\text{D}]^{2+}$ , with both ions being complexed with two 18-crown-6 molecules. When comparing those spectra with the spectra of their uncomplexed counterparts, it can be observed that the spectra of complexed species show a significantly altered spectral structure in both, the amide-I and -II region. Slightly narrower lines can be expected, as fewer absorbed photons are required to fragment this complex. Most striking in the amide-I region is that the peak near  $1600\text{ cm}^{-1}$  has a much lower intensity (and even completely absent for the deuterated complex). In that region, contributions from  $\text{C}=\text{O}$  oscillators involved in strong hydrogen bonds as well as from  $-\text{NH}_3^+$   $\delta_{\text{as}}$  modes would be expected. The crown-ether probably shields the  $-\text{NH}_3^+$  groups from interacting and forming strong hydrogen bonds with backbone  $\text{C}=\text{O}$  groups. Thus we can assign a large fraction of the intensity near  $1600\text{ cm}^{-1}$  in the spectra of the uncomplexed ions to  $\text{C}=\text{O}$  groups involved in such an interaction. Additional deuteration also shifts the  $-\text{NH}_3^+$   $\delta_{\text{as}}$  mode outside the experimental range. This is in line with the reduction in intensity near  $1600\text{ cm}^{-1}$  in the spectrum of  $[\text{GramS} + 2\text{H}]^{2+}$  and the total absence of intensity in that range in the spectrum of deuterated  $[\text{d-GramS} + 2\text{D}]^{2+}$  complexed with 18-crown-6. In the amide-II region around  $1500\text{ cm}^{-1}$ , the situation is more complex. There, deuteration changes the nature of the modes from predominantly  $\text{N}-\text{H}$  bending to  $\text{N}-\text{C}$  stretching upon deuteration. Concomitant with that is a change in relative intensity, compared to the amide-I mode. In addition, the  $-\text{NH}_3^+$   $\delta_{\text{s}}$  mode is shifted to lower wavenumber. Also, the complexation with 18-crown-6 might affect both the positions and intensities of the  $-\text{NH}_3^+$   $\delta$  modes. All those factors make the interpretation of the amide-II region difficult.

## Calculations

To learn more about the structure of gas-phase  $[\text{GramS} + 2\text{H}]^{2+}$ , different conformeric structures and their IR spectra were calculated. There are two fundamental problems that need to be addressed. First, the conformational space is very large and it is difficult to select possible candidate structures for further investigations. Second, even when reasonable candidate structures are found, their structures need to be optimized, and the energies as well as the IR spectra need to be calculated. For the calculations of IR spectra of small peptides containing only a few amino acids, DFT methods have been shown to give at least reasonable geometries and IR spectra.<sup>14</sup> For species of the size of  $[\text{GramS} + 2\text{H}]^{2+}$ , DFT methods are, however, computationally expensive.

We choose a molecular dynamics (MD) based search scheme described below to find candidate structures which are then further investigated at the B3LYP level with the def-SVP basis

(39) Julian, R. R.; Beauchamp, J. L. *J. Am. Soc. Mass Spectrom.* **2002**, *13*, 493–498.

set using Turbomole<sup>40</sup> with the ri-approximation. The MD calculations are performed with the Amber 9<sup>41</sup> program using the ff96 force field.<sup>42</sup> The parameters for the nonstandard amino acid ornithine are adapted from parameters of lysine by removing one CH<sub>2</sub> group and distributing its net charge to the neighboring atoms. To efficiently sample the conformational space, replica exchange molecular dynamics (REMD)<sup>43</sup> has been performed on 16 parallel runs with temperatures ranging in a geometric series from 270 to 800 K. Time steps are set to one femtosecond, replica exchange attempts occur every picosecond and the total length of each simulation is 100 ns.

At each simulation, 1000 structure snapshots from the trajectory at 312 K are picked and further analyzed. First, the structures are energy minimized at the force field level. Next, they are grouped in families of structural similarity. This is done by using the rms atom displacement (rmsd) values between two structures to judge the similarity between them. In the calculations of the rmsd values, all atoms of the peptidic backbone plus the N–H hydrogen as well as the –NH<sub>3</sub><sup>+</sup> nitrogen on the ornithine side-chains are used. The rmsd values are then calculated between all pairs of structures. Those values are plotted in a two-dimensional color coded matrix and this matrix is sorted by grouping species with low rmsd values such that blocks with similar structures appear. From each block, several low energy structures are taken, their energies minimized at the B3LYP level and the IR spectra calculated using numerical differentiation.

From the calculations on [GramS + 2H]<sup>2+</sup>, visual inspection shows that for most structures, the dominant interaction occurs between the –NH<sub>3</sub><sup>+</sup> group of the Orn side-chain and the C=O groups of the Phe, Orn, Val and Pro amino acids. In general, there are two possibilities for such interactions. The Orn side-chains can either coordinate to the backbone C=O groups that are found clockwise or counterclockwise (see Figure 1), that is, the side-chain on top orients to the right and the one below to the left (clockwise) or *vice versa*. For an interchange between those two orientations, both side-chains have to act concertedly and at least four, presumably strong, hydrogen bonds have to be broken. Consequently, the barrier for such a transition is expected to be high. For that reason, two separate simulations were started, one with the Orn side-chains oriented clockwise and one with counterclockwise orientation.

From the resulting 2000 structures, 21 were selected for further investigations using B3LYP. Ten structures had a counter-clockwise and eleven a clockwise Orn side-chain orientation. Interestingly, the structure with the lowest B3LYP energy is also the one which has the lowest ff96 energy. The relative ff96 and B3LYP energies can be compared, by setting the lowest energy structure as the zero energy in both sets. For the ten counter-clockwise structures, the rms difference in relative energy between ff96 and B3LYP is 11 kcal/mol, for the eleven clockwise structures 7 kcal/mol. An inspection of those 21 structures resulted in five low energy families and the lowest energy structure of each of those families together with

the calculated IR spectra is shown in Figure 3. Note that the structures in Figure 3 are turned upside down, compared to the structure in Figure 1. The main structural differences result from differences in hydrogen bonding of the Orn side-chains with the backbone. Spectra for hydrogenated and deuterated species are shown on the left-hand and right-hand side, respectively. The frequency positions in all calculated spectra as well as in the further discussion are scaled by 0.9614.<sup>44</sup>

The top two structures are characterized by a clockwise (see Figure 1) orientation of the Orn side-chains. In case of the top structure (A), the Orn side-chains coordinate to the C=O groups from their own residue as well as Phe C=O groups two residues away. The structure is very symmetric and distances between the H-atoms on the –NH<sub>3</sub><sup>+</sup> groups and the O-atoms of the corresponding C=O groups are 1.68 and 1.73 Å to Phe and Orn, respectively. Four  $\beta$ -sheet type interactions are present and H-bonding distances are 2.06 and 1.95 Å for the outer two and inner two H-bonds, respectively. In addition, the Phe aromatic rings are closely coordinated to the charged side-chains. At both the ff96 and the B3LYP level, this structure is found to be lowest in energy. The structure shown in the second row (B) is also based on a clockwise orientation of the Orn side-chains, this time however interacting with the C=O groups of the Phe and Pro residues (distances of 1.63 and 1.84 Å, respectively). Four  $\beta$ -sheet type interactions are present as well with 2.31 and 2.01 Å as distances for the outer and inner ones, respectively. At the B3LYP level, this structure is 7.2 kcal/mol higher in energy than structure A.

The three structures shown in the lower part of Figure 3 (C–E) all have counter-clockwise orientations of the Orn side-chains. In structure C, the Orn side-chains are coordinated to C=O groups of the Phe, Orn (opposite side) and Val (next to the Orn group) residues. The distances between the H-atoms on the –NH<sub>3</sub><sup>+</sup> groups and the O-atoms of the corresponding C=O groups range from 1.62 Å to 1.87 Å. The only other –H...O = distances closer than 2.5 Å are found between the two Leu C=O and corresponding Val N–H groups. Such interactions are expected for a  $\beta$ -sheet type structure. The distances between the corresponding atoms are with 2.18 and 2.22 Å relatively large, however. In relative energy, this structure is 1.4 kcal/mol higher in energy than A. Structure D on the second row from below is similar to structure C. There as well, one Orn side-chain coordinates to Phe, Orn and Val residues. The other Orn side-chain coordinates to a Phe and an Orn residue as well as to the aromatic ring of the Phe residue. The H-bond lengths are similar to the ones found in C; H-bonds in which the Orn side-chains are involved range from 1.60 Å to 1.87 Å and for the two  $\beta$ -sheet type interactions, H-bond lengths of 2.22 and 2.29 Å can be found. In addition, a weak C<sub>7</sub> type interaction with a distance of 2.37 Å can be noted between a Pro C=O and a Orn N–H. The relative energy of D is +6.2 kcal/mol.

The structure shown at the bottom (E) is very symmetric and characterized by interactions of the two Orn side-chains with the Phe and Pro residues. The distance to the Phe C=O is 1.67 Å and to the Pro C=O 1.83 Å. In this structure, four  $\beta$ -sheet type interactions are present. The distances for the outer H-bonds is 2.04 Å and for the inner H-bonds 1.84 Å. The Orn C=O groups have their closest H-bonding interaction with the Orn N–H in a C<sub>5</sub> type interaction. The distance is, however, with 2.96 Å large and the corresponding interaction, thus, weak. The

(40) TURBOMOLE V6.0 2009, a development of University of Karlsruhe and Forschungszentrum Karlsruhe GmbH, 1989–2007, TURBOMOLE GmbH, since 2007; available from <http://www.turbomole.com>.

(41) Case, D. *AMBER 9*; University of California: San Francisco, 2006.

(42) Kollman, P.; Dixon, R.; Cornell, W.; Fox, T.; Chipot, C.; Pohorille, A. *Computer Simulation of Biomolecular Systems*; Elsevier: New York, 1997; Vol. 3, pp 83–96.

(43) Mitsutake, A.; Sugita, Y.; Okamoto, Y. *Biopolymers* **2001**, *60*, 96–123.

(44) Scott, A.; Radom, L. *J. Phys. Chem.* **1996**, *100*, 16502–16513.

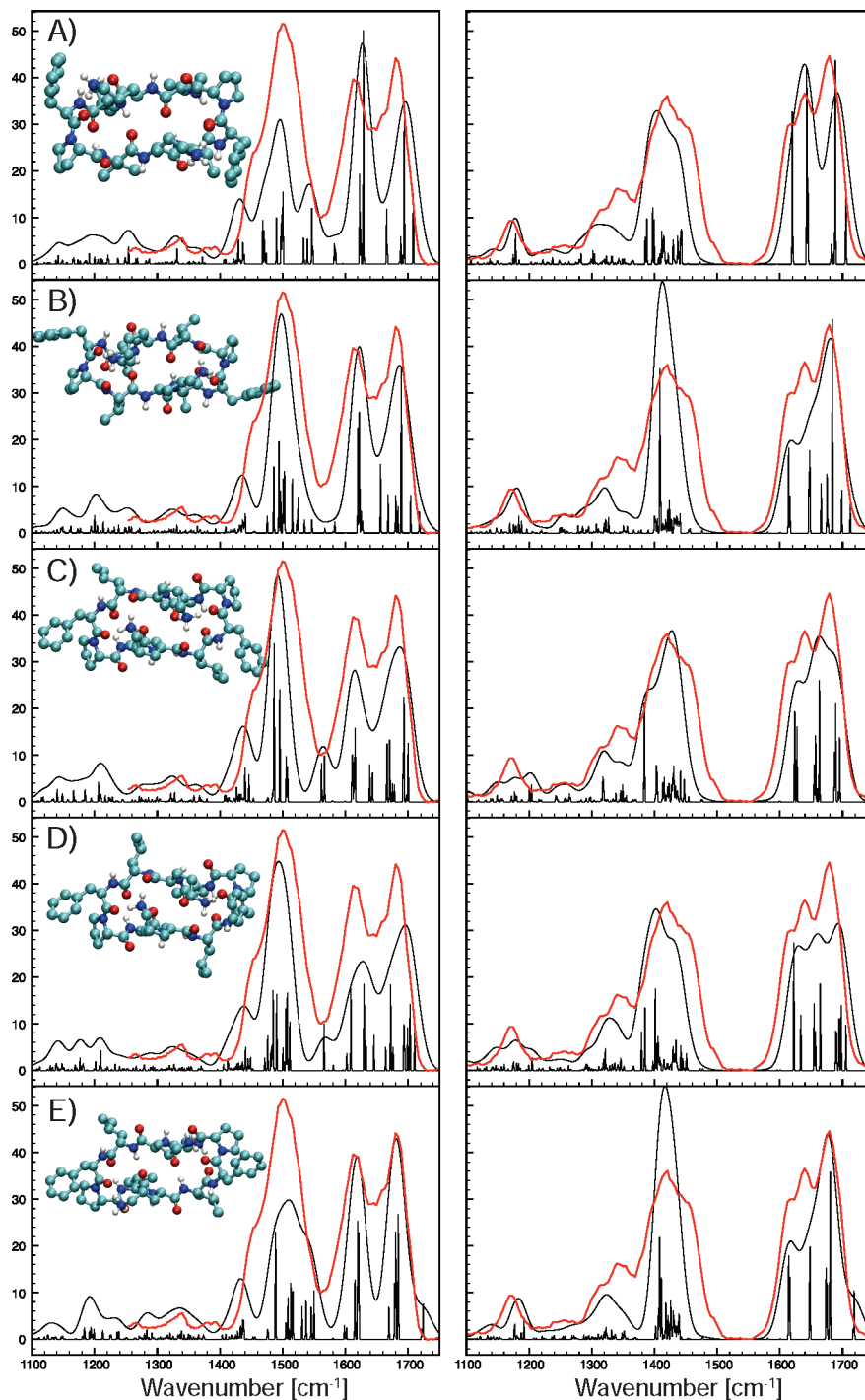


**Figure 3.** Experimental IR spectra of  $[\text{GramS} + 2\text{H}]^{2+}$  and perdeuterated  $[\text{d-GramS} + 2\text{D}]^{2+}$  (red solid line, left and right part respectively) compared to theoretical predictions for five calculated structures. The sharp spectra result from a convolution of the theoretical stick spectrum with a  $1\text{ cm}^{-1}$  full width Gaussian and the broader spectra in black from a convolution with a 2% full width Gaussian. All calculated line positions are scaled by 0.9614.

relative energy of E is with  $+15.7\text{ kcal/mol}$  the highest of the five structures considered.

When comparing the calculated IR spectra to the experimental ones, many of the general features shown in the experiment are reproduced. A perfect agreement, however, is not observed for any of the calculated structures. In order to characterize the observed spectrum, it is instructive to analyze the normal modes in the calculated spectrum. For the following, we would like to discuss the normal modes in the amide-I region of the deuterated structures A and C. For deuterated A in the range between  $1600$  and  $1720\text{ cm}^{-1}$ , the

calculated spectrum in 3 shows four groups of peaks. At the lowest frequency two almost degenerate vibrations at  $1620\text{ cm}^{-1}$  resulting from Phe C=O stretch motion occur. Next higher at  $1643\text{ cm}^{-1}$  and  $1645\text{ cm}^{-1}$ , C=O stretching vibrations of the two Orn C=O groups are present. The four vibrations of the  $\beta$ -sheet Leu and Val C=O groups are found between  $1681\text{ cm}^{-1}$  and  $1688\text{ cm}^{-1}$ . At the highest frequency at  $1705\text{ cm}^{-1}$  and  $1706\text{ cm}^{-1}$ , vibrations of the Pro C=O groups are found. Qualitatively, those shifts can be understood by having the C=O groups with the strongest H-bonds (bond to the charged Orn side-chain) most to the red, the

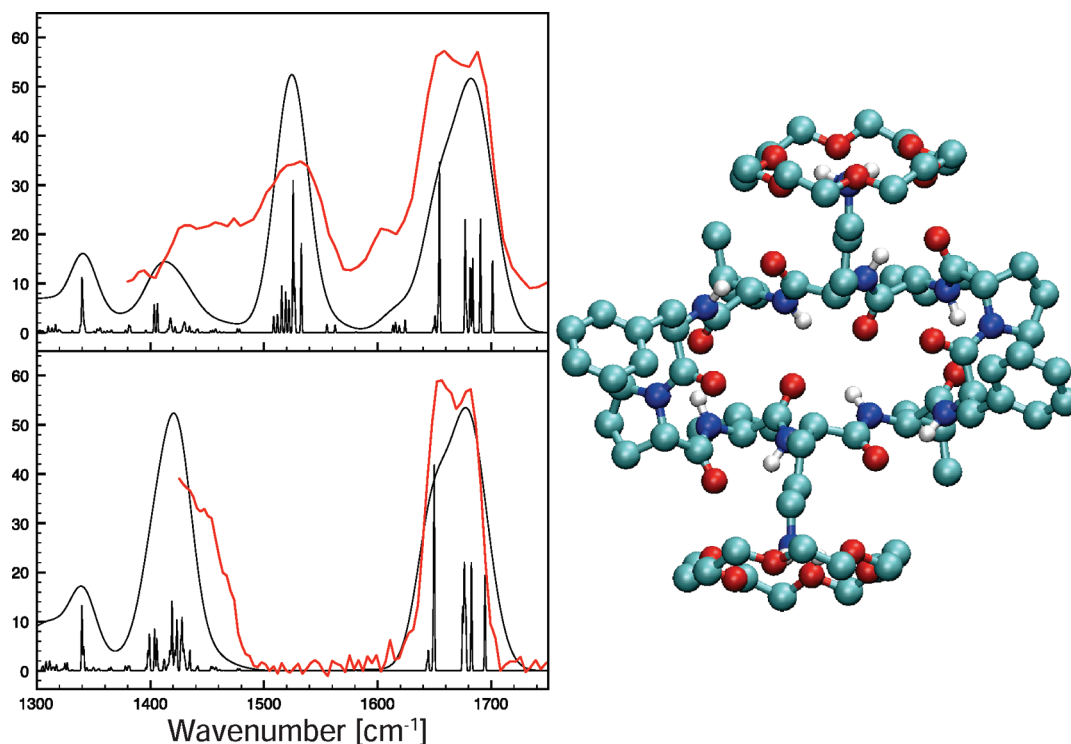


**Figure 4.** Experimental IR spectra of  $[\text{GramS} + 2\text{H}]^{2+}$  and perdeuterated  $[\text{d-GramS} + 2\text{D}]^{2+}$  complexed with two 18-crown-6 molecules (red solid line, top and bottom, respectively) compared to a theoretical prediction. The sharp spectra result from a convolution of the theoretical stick spectrum with a  $1\text{ cm}^{-1}$  full width Gaussian and the broader spectra in black from a convolution with a  $2\%$  full width Gaussian. All calculated line positions are scaled by  $0.9614$ .

medium strongly H-bonded  $\beta$ -sheet groups more to the blue and the essentially non H-bond Pro vibrations most to the blue.

For the deuterated structure shown in Figure 3C, ten vibrational modes, all stemming from C=O stretching vibrations, are found in the region between  $1600$  and  $1700\text{ cm}^{-1}$ . Most to the red, at  $1624$  and  $1628\text{ cm}^{-1}$ , vibrations of the two Phe C=O groups occur. The Val C=O vibrations are found at  $1655$  and  $1657\text{ cm}^{-1}$ , followed by the Orn C=O vibrations at  $1660$  and  $1663\text{ cm}^{-1}$ . Between  $1687$  and  $1695\text{ cm}^{-1}$ , the Leu and Pro C=O vibrations are found which appear rather mixed. As in the case of the vibrational modes of structure A), the red shift qualitatively follows the strength of H-bonding. Most to the red, modes of groups are found that (strongly) interact with the charged Orn side-chain, while the vibrations of the more weakly H-bonded Leu and Pro C=O groups are found on the blue side of the peak.

Structures and spectra for  $[\text{GramS} + 2\text{H}]^{2+}$  complexed with two 18-crown-6 molecules were calculated using the same methodology that was employed for uncomplexed  $[\text{GramS} + 2\text{H}]^{2+}$ . At the ff96 level, four structural families are found and a total of nine structures were optimized and their IR spectra calculated at the B3LYP level. In all structures that were found, the 18-crown-6 molecules are tightly coordinated to the Orn side-chains. In three of the four families, in addition some coordination of C=O groups toward the Orn  $-\text{NH}_3^+$  groups is observed. This, however, comes at the expense of intramolecular H-bonding and at the B3LYP level, the lowest energy structure from those families is  $12.8\text{ kcal/mol}$  higher in energy than the overall lowest energy structure. Figure 4 shows this overall lowest energy structure, together with the calculated IR spectra for protonated and deuterated species. The structure is characterized by Orn side-chains coordinating 18-crown-6 molecules and

pointing away from the peptide backbone. The Leu and Val C=O groups are found to be involved in  $\beta$ -sheet type H-bonding with distances for the outer Leu C=O H-bond of  $2.00\text{ \AA}$  and for the inner Val C=O H-bond of  $2.37\text{ \AA}$ . The latter C=O groups, however, have with  $2.20\text{ \AA}$  shorter distances to the neighboring Leu N-H groups to form  $C_7$  type H-bonds. The Pro and Orn C=O groups form  $C_7$  type H-bonds with the adjacent Orn and Phe N-H groups at distances of  $2.09$  and  $2.00\text{ \AA}$ , respectively. Only the Phe C=O groups have no close H-bonding partner.

Qualitatively, the calculated spectra are in good agreement with the ones obtained experimentally. For the nondeuterated molecule, both the peaks in the amide-I and -II region are predicted narrower than observed. For the deuterated species, the width of the amide-I peak is well reproduced. Unfortunately, for this molecule, the measurements did not cover the amide-II region. For the amide-I peak, the splitting which is experimentally observed for the protonated as well as the deuterated species is not reproduced by the calculations.

Visualizing the vibrations in the amide-I region for the deuterated species shows that most of the Orn C=O vibrations are present most to the red, at  $1643$  and  $1644\text{ cm}^{-1}$ . They are, however, of low IR intensity. Pro C=O vibrations are predicted to be much stronger and are found at  $1649$  and  $1650\text{ cm}^{-1}$ . Significantly shifted to the blue, at  $1675$  and  $1676\text{ cm}^{-1}$ , Leu " $\beta$ -sheet" vibrations occur. They are to some extent mixed with the vibrations of the Phe C=O groups which are found at  $1677$  and  $1678\text{ cm}^{-1}$ . Most to the blue are the out-of-phase and in-phase combinations of the Val C=O groups at  $1682$  and  $1694\text{ cm}^{-1}$ . Such a splitting might be indicative of different environments. Then, however, localized modes would be expected. In the present case, the two C=O groups are in very similar environments and as they are quite close to each other, they

couple and give rise the mentioned in- and out-of-phase vibrations. In conclusion for  $[\text{GramS} + 2\text{H}]^{2+}$  complexed with two 18-crown-6 molecules, it can be noted that, contrary to expectations, the red part of the amide-I peak results from Orn and Pro C=O vibrations while the Leu and Val C=O vibrations are rather found near the blue at around  $1680\text{ cm}^{-1}$ .

## Discussion

The experimental results clearly show the importance of the Orn  $-\text{NH}_3^+$  side-chain interaction on the IR spectra, and, thus, also on the structure of gas-phase gramicidin S. The deuteration experiments show that the red shoulder in the experimental amide-I peak is caused by  $-\text{NH}_3^+$  umbrella motion and further, that this mode couples to other C=O stretching modes, as the amide-I peak shape changes upon deuteration of the molecule. Further evidence for the  $-\text{NH}_3^+$ -peptide backbone interactions comes from the 18-crown-6 experiments, which demonstrate that the red side of the amide-I peak is due to oscillators that interact with the  $-\text{NH}_3^+$  group. The calculations shed further light on the nature of these side-chain - backbone interactions. In all calculated structures, a  $-\text{NH}_3^+$ -Phe C=O interaction is found to be strong, irrespective whether the orientation of the side-chain occurs clockwise or counterclockwise. In addition, an interaction with the Orn C=O is present in the low energy structures A, C and D presented in Figure 3. An interaction with Val C=O is predicted for C and D and with Pro C=O for B and E. Due to their strong H-bonded nature, these strongly H-bonded Phe, Val, Pro or Orn C=O groups give rise to the resonances which are found most to the red in the amide-I peak. Leu C=O groups on the other hand do not interact with the Orn  $-\text{NH}_3^+$  side-chains. Instead, they are found to bind to the opposing Val N-H groups in a  $\beta$ -sheet type arrangement. Their vibrations, however, are predicted in calculations for structures A) and C) in Figure 3 and for the crown-ether complexed structure in Figure 4 to occur on the blue side of the amide-I peak between  $1675$  and  $1695\text{ cm}^{-1}$ . When the Val C=O is coordinated to an  $-\text{NH}_3^+$ , its resonance is predicted to be found around  $1656\text{ cm}^{-1}$  (see Figure 3C). When this is not the case and the Val C=O groups interacts with an opposing Leu N-H groups in a  $\beta$ -sheet arrangement (see Figure 3A) and Figure 4, its resonances are found to be close to that of Leu C=O " $\beta$ -sheet" in gramicidin S between  $1682$  and  $1694\text{ cm}^{-1}$ .

When comparing the experimental spectra with the calculated ones, all calculations give reasonable agreements between theory and experiment. In the experiment, the amide-I band appears to consist of two components for the hydrogenated gramicidin S and of three for the deuterated species. In all calculations a splitting of the amide-I band is predicted as well. There are, however, also differences in the calculated and experimental relative intensities of the amide-I components, and it is difficult to decide which of the structures in Figure 3 gives the best match to experiment. Theory calculates spectra at 0 K. The experiment on the other hand does not measure the linear IR absorption spectrum of a fully annealed sample at 0 K, but is rather measured as an IRMPD spectrum. For many species, it was shown that IRMPD spectra can be quite similar to the corresponding linear absorption spectra.<sup>37</sup> The experimental IRMPD spectrum is linearly corrected for the variation in FEL power over the tuning range. This is however only a first order approximation and errors in relative intensities may result.

In addition to uncertainties in relative intensities, peak positions can also deviate from their positions in a linear, 0 K spectrum. This can be caused by mode anharmonicities, in

combination with the IRMPD mechanism<sup>37</sup> and the fact that the excitation starts from a room temperature sample. However, one can estimate the resulting shifts to be on the order of a few wavenumbers,<sup>37</sup> thus relatively small compared to the widths of the observed resonances.

Another complication stems from the possibility of the presence of more than one conformer. The presence of different conformers of gas-phase  $[\text{GramS} + 2\text{H}]^{2+}$  is observed in recent low temperature experiments.<sup>45</sup> Ion mobility experiments at 300 K on the other hand did not indicate the presence of different conformers with vastly different overall shapes.<sup>34</sup> We have calculated cross sections for the structures presented in Figure 3. The results show that structure A has the lowest cross-section (highest mobility) and, for example, structure E has an about 10% higher cross-section. Such a difference could stem from differences in the orientations of the rather flexible phenyl side-chains and, in a 300 K experiment, thermal motion might average out those deviations to some extent. Indeed, performing cross-section calculations on structures where the phenyl groups are deleted reduces the differences in relative cross sections to about 5%. With the addition of thermal motion of the other side-chains, the resulting differences in mobilities might be insufficient to be observable in most ion mobility experiments. In the calculations, many local minima were populated. It is also observed, that in the simulations, transition from a clockwise to counterclockwise (or *vice versa*) side-chain orientation occurred only infrequently with a high barrier between those two nearly isoenergetic conformational spaces. It is thus likely that in the experiment, a distribution of different conformers is present and the resulting IRMPD spectrum would, consequently, be a superposition of several spectra. A possible indication for this is that our observed amide-II band is significantly broader than calculated.

Doubly protonated gramicidin S in the gas phase might thus not be a good model system for an isolated  $\beta$ -sheet peptide, as the  $\beta$ -sheet can be disturbed by side-chain-backbone interactions. However, the spectrum of  $[\text{GramS} + 2\text{H}]^{2+}$  complexed with two 18-crown-6 molecules might be expected to resemble more closely that of an unperturbed antiparallel pleated  $\beta$ -sheet conformation. There, the amide-I peak appears to consist of two components, one near  $1653\text{ cm}^{-1}$  and one near  $1680\text{ cm}^{-1}$ . Gramicidin S in solution shows a band at  $1629\text{ cm}^{-1}$  when dissolved in  $\text{D}_2\text{O}$ , which shifts to  $1652\text{ cm}^{-1}$  when DMSO is used as a solvent.<sup>18</sup>  $\text{D}_2\text{O}$  is a polar and protic solvent which can solvate the charged side-chains and can be involved in H-bonding to the six C=O groups and four N-H groups which are not part of the  $\beta$ -sheet section of the molecule. DMSO is a polar but aprotic solvent, which can solvate the charged side-chains, but which is, however, less effective in H-bonding. The situation in DMSO could thus be quite comparable to the situation when the charged side-chains are complexed with 18-crown-6. This is in line with our observation that the redmost peak in the amide-I band of gramicidin S occurs at essentially the same frequency. However, a comparison between experiment and theory indicates that this redmost part is not caused by the  $\beta$ -sheet C=O groups but rather by the Orn and Pro C=O groups and that the Val and Leu C=O groups contribute more to the blue part near  $1680\text{ cm}^{-1}$ .

For proteins in the condensed phase, amide-I vibrations of  $\beta$ -sheet molecules are observed near  $1633\text{ cm}^{-1}$ .<sup>16</sup> Small gas-phase  $\beta$ -sheet model systems show amide-I resonances that are

(45) Nagornova, N.; Rizzo, T.; Boyarkin, O. unpublished.

all above  $1650\text{ cm}^{-1}$ <sup>15</sup> and it has been pointed out, that a classification of the structure just based on the position of amide-I resonances is not possible for those systems.<sup>15</sup> However, it is also conceivable that the condensed phase value of  $1633\text{ cm}^{-1}$  is applicable only for  $\beta$ -sheet sections that interact strongly with their surroundings, such as  $\beta$ -sheet sections that are embedded in larger protein structures or  $\beta$ -sheet sections that are part of an amyloid network. For isolated  $\beta$ -sheet sections, the  $1633\text{ cm}^{-1}$  value might not apply. In line with that is the observation that for  $\beta$ -sheet sections that interact only with polar solvents, a shifted value of  $1640\text{ cm}^{-1}$  can be observed, however at high concentrations, when aggregation takes place, a new peak at  $1616\text{ cm}^{-1}$  is observed.<sup>17</sup> The FTIR studies on gramicidin S dissolved in various solvents,<sup>18</sup> the data on small  $\beta$ -sheet model systems<sup>15</sup> as well as the data presented here indicate that the intrinsic frequency of  $\beta$ -sheet peptides might be substantially to the blue, more in the range  $1650\text{--}1680\text{ cm}^{-1}$ .

For helical or random coil systems, the dependence on the environment might be less pronounced. In an isolated  $\beta$ -hairpin, only half of the C=O and N-H groups have a partner to interact with and the other half has to interact with either the environment or has to interact intramolecularly via weak C<sub>5</sub> hydrogen bonding. In helices, on the other hand, only the terminal C=O or N-H groups do not have a partner. In agreement with that is the observation that for cytochrome C in the gas phase, which has most likely a predominantly random coil or helical structure, an amide-I band between  $1660$  and  $1670\text{ cm}^{-1}$ <sup>17</sup> is observed close to the value in the condensed phase.<sup>46</sup>

## Conclusions

The mid-infrared spectrum of the doubly protonated (deuterated) gas-phase peptide gramicidin S has been measured at

$300\text{ K}$  using IRMPD in an FTICR cell. The spectra show a broad split peak between  $1580$  and  $1720\text{ cm}^{-1}$ . A comparison to theory shows the importance of the interactions of the charged side-chains with the backbone, which is responsible for the lower frequency part of the amide I peak. When this interaction is inhibited via complexation with two 18-crown-6 molecules, the amide I peak narrows and shows two maxima at  $1653$  and  $1680\text{ cm}^{-1}$ . A comparison to calculations shows that for this complexed ion, four C=O groups are in an antiparallel  $\beta$ -sheet arrangement. The data thus represents the first evidence for the stability of a charged  $\beta$ -sheet peptide in the gas phase. An analysis of the calculated spectra shows that those  $\beta$ -sheet C=O groups give rise to the vibrations near  $1680\text{ cm}^{-1}$ , in contrast to expectations based on values for the condensed phase, where resonances of  $\beta$ -sheet sections are thought to occur near  $1630\text{ cm}^{-1}$ . The difference between those values may be caused by interactions with the environment, as the condensed phase value is mostly deduced for  $\beta$ -sheet sections that are embedded in larger proteins, that interact strongly with solvent or that are part of partially aggregated species.

**Acknowledgment.** We gratefully acknowledge the support by the “Stichting voor Fundamenteel Onderzoek der Materie” (FOM) in providing the required beam time on FELIX and highly appreciate the skillful assistance by the FELIX staff, in particular Dr. B. Redlich and Dr. AFG van der Meer. We thank Prof. A.S. Ulrich and Dr. P. Wadhvani for making the gramicidin S sample available to us. Further, we like to thank Prof. T. Rizzo and Dr. O. Boyarkin for communicating experimental data prior to publication.

**Supporting Information Available:** Calculated structures, calculated IR spectra and full citation for ref 41. This material is available free of charge via the Internet at <http://pubs.acs.org>.

JA909842J

(46) Speare, J. O.; Rush, T. S. *Biopolymers* **2003**, *72*, 193–204.